

# Geophysical Research Letters®



## RESEARCH LETTER

10.1029/2024GL110871

### Key Points:

- 10,800-year-long, 3-year-resolution, warm-season temperature reconstruction from biochemical varves from Lake Żabińskie, Poland
- Peak summer temperatures occurred during the early Holocene with declining summer insolation driving cooling during the past 8,000 years
- The rate of modern warming is highly unusual, at least 4 standard deviations above the mean temperature trend of the past 10,800 years

### Supporting Information:

Supporting Information may be found in the online version of this article.

### Correspondence to:

P. D. Zander,  
zander3@lnl.gov

### Citation:

Zander, P. D., Żarczyński, M., Tylmann, W., Vogel, H., & Grosjean, M. (2024). Subdecadal Holocene warm-season temperature variability in central Europe recorded by biochemical varves. *Geophysical Research Letters*, 51, e2024GL110871. <https://doi.org/10.1029/2024GL110871>

Received 17 JUN 2024

Accepted 3 SEP 2024

### Author Contributions:

**Conceptualization:** Paul D. Zander, Maurycy Żarczyński, Wojciech Tylmann, Martin Grosjean

**Data curation:** Paul D. Zander, Maurycy Żarczyński, Wojciech Tylmann

**Formal analysis:** Paul D. Zander, Maurycy Żarczyński

**Funding acquisition:** Paul D. Zander, Wojciech Tylmann, Martin Grosjean

**Investigation:** Paul D. Zander, Maurycy Żarczyński, Wojciech Tylmann, Hendrik Vogel

**Methodology:** Paul D. Zander, Maurycy Żarczyński

© 2024. The Author(s).

This is an open access article under the terms of the [Creative Commons Attribution-NonCommercial-NoDerivs License](https://creativecommons.org/licenses/by/4.0/), which permits use and distribution in any medium, provided the original work is properly cited, the use is non-commercial and no modifications or adaptations are made.

## Subdecadal Holocene Warm-Season Temperature Variability in Central Europe Recorded by Biochemical Varves

Paul D. Zander<sup>1,2,3</sup> , Maurycy Żarczyński<sup>4,5</sup> , Wojciech Tylmann<sup>5</sup>, Hendrik Vogel<sup>6</sup>, and Martin Grosjean<sup>2</sup> 

<sup>1</sup>Climate Geochemistry Department, Max Planck Institute for Chemistry, Mainz, Germany, <sup>2</sup>Institute of Geography, Oeschger Centre for Climate Change Research, University of Bern, Bern, Switzerland, <sup>3</sup>Now at Center for Accelerator Mass Spectrometry, Lawrence Livermore National Laboratory, Livermore, CA, USA, <sup>4</sup>School of Earth and Sustainability, Northern Arizona University, Flagstaff, AZ, USA, <sup>5</sup>Faculty of Oceanography and Geography, University of Gdansk, Gdansk, Poland, <sup>6</sup>Institute of Geological Sciences, Oeschger Centre for Climate Change Research, University of Bern, Bern, Switzerland

**Abstract** Paleoclimate data provide important information about the character of natural climate variability. However, records with sufficient length and resolution to resolve high-frequency (decadal-scale) variability across the Holocene are scarce. We present a 10,800-year reconstruction of spring and summer temperature at three-year resolution based on biochemical varves from Lake Żabińskie, Poland. The reconstruction is based on Ca/Ti ratio, which are significantly correlated with instrumental spring and summer temperature spanning 240 years. Major climate events of the Holocene period are represented in the reconstruction, including the Holocene Thermal Maximum, 8.2 ka Event, Medieval Climate Anomaly, and Little Ice Age. A low-frequency 8,000-year decreasing trend in warm-season temperatures is driven by declining summer insolation. Temperature variability is highest during the early Holocene, likely related to warmer and drier conditions. The rate of warming during the past 90 years is extremely unusual, if not unprecedented for the Holocene, based on our reconstruction.

**Plain Language Summary** Studying past climate change helps us understand how the climate system works. One aspect of past climate that is not well understood is how much temperatures changed from year to year and over decades during warm periods of Earth's history. In this study, we measured chemical properties of lake sediments from Poland and found that chemical changes were related to spring and summer temperature changes. We used this data to estimate spring and summer temperatures during the past 10,800 years. Relatively warm summers occurred around 9,000–7,500 years ago, a period known from other studies to be relatively warm in the northern hemisphere. We also found greater variability in temperatures during this warm period. Our long record of spring and summer temperatures shows that the warming rate of the past 90 years is most likely faster than any time during the past 10,800 years, showing that human-caused global warming is more extreme than natural climate variations.

## 1. Introduction

The study of temperature variations during the geologic past is important for understanding the processes that control climate over a variety of timescales. Temperature variability during the Holocene (11,700 years BP to present) has been studied intensively, yet major questions remain unresolved. For example, the Holocene Temperature Conundrum (Kaufman & Broadman, 2023; Liu et al., 2014) refers to the discrepancy in long-term trends between climate model simulations and proxy data. Models typically show a long-term warming trend toward the present during the Holocene (Erb et al., 2022; Liu et al., 2009), whereas proxy data suggest that temperatures peaked during the early-to-mid-Holocene Thermal Maximum (HTM), and subsequently declined (Kaufman, McKay, Routson, Erb, Dätwyler, et al., 2020; Marcott et al., 2013). The debate surrounding the Holocene Temperature Conundrum revolves around the seasonal signal of temperature recorded in proxies as well as the regional nature of the HTM (Bova et al., 2021; Cartapanis et al., 2022; Erb et al., 2022; Kaufman & Broadman, 2023; Liu et al., 2014).

Interannual- to multidecadal-scale temperature variability remains poorly constrained during the Holocene. In the Temp12k temperature database (Kaufman, McKay, Routson, Erb, Davis, et al., 2020), only 49 of 1,319 proxy

**Project administration:**

Wojciech Tylmann, Martin Grosjean

**Resources:** Wojciech Tylmann,  
Martin Grosjean

**Software:** Paul D. Zander

**Supervision:** Wojciech Tylmann,  
Martin Grosjean

**Validation:** Paul D. Zander

**Visualization:** Paul D. Zander,  
Maurycy Żarczyński

**Writing – original draft:** Paul D. Zander

**Writing – review & editing:**

Maurycy Żarczyński, Wojciech Tylmann,  
Hendrik Vogel, Martin Grosjean

records have an average time resolution of 20 years or less. High-resolution records are required to assess the frequency of extreme events and to characterize amplitudes and trends of natural variability at (sub)decadal scales. The lack of temperature reconstructions with decadal or better resolution makes it challenging to compare proxy estimates of high-frequency variability to model simulations (Essell et al., 2023). Given that summer temperature variability and extremes have increased in Europe in recent decades and are projected to continue to increase due to anthropogenic climate change (Seneviratne et al., 2006), understanding high-frequency temperature variability during past warm periods, such as the HTM, is an important paleoclimate target.

Varved lake sediments are well-suited for capturing high-frequency climate variations because it is possible to obtain proxy measurements that are seasonally resolved (Brauer et al., 2009; Zolitschka et al., 2015), particularly through the use of rapid, non-destructive, high-resolution scanning and imaging methods such as micro-X-ray fluorescence ( $\mu$ XRF) (Bertrand et al., 2023). Quantitative temperature reconstructions with subdecadal resolution have been produced from varved sediments (e.g., Lapointe et al., 2020; Stewart et al., 2011; Trachsel et al., 2008); however, Holocene-length reconstructions remain scarce.

Previous work at Lake Żabińskie, Poland demonstrated links between seasonal meteorologic conditions and the properties of biochemical varves (Zander, Żarczyński, Tylmann, et al., 2021; Żarczyński et al., 2022). In particular, calcite precipitation is strongly influenced by air temperatures in the spring and summer. We hypothesize that Ca/Ti (calcium/titanium) ratios (a proxy for endogenic calcite precipitation) can be used to quantitatively reconstruct warm-season temperatures in the past at Lake Żabińskie. We use a calibration-in-time approach (von Gunten et al., 2012) to estimate temperatures at three-year resolution over the past 10,800 years. The reconstruction provides valuable information about temperature variability at subdecadal to millennial timescales through the Holocene.

## 2. Methods

### 2.1. Study Site

Lake Żabińskie, Poland (54.1318° N, 21.9836° E; Figure 1) is a post-glacial, eutrophic, hardwater lake that is deep (44.4 m) compared to its area (0.42 km<sup>2</sup>). The catchment geology is glacial tills and fluvioglacial deposits (Szumański, 2000). Modern (1991–2020) monthly temperatures range from  $-2.5^{\circ}\text{C}$  in January to  $18^{\circ}\text{C}$  in July (Tomczyk & Bednorz, 2022). Temperatures at this site are representative of the Baltic region and much of central and eastern Europe (Figure 1a). Limnological and sediment trap monitoring have been conducted regularly since 2012 (Tylmann et al., 2023). Thermal stratification and prolonged periods of anoxic conditions in the hypolimnion facilitate the preservation of biochemical varves (Bonk, Tylmann, Amann, et al., 2015; Żarczyński et al., 2022).

### 2.2. Chronology

The Lake Żabińskie sediment chronology is based on previously published varve counts and radiocarbon ages on terrestrial macrofossils (Bonk, Tylmann, Goslar, et al., 2015; Zander et al., 2020; Zander, Żarczyński, Tylmann, et al., 2021; Zander, Żarczyński, Vogel, et al., 2021; Żarczyński et al., 2018). The sediments are composed of carbonate- and organic-rich mud, and varves are preserved in almost the entirety of the 10,800-year record (Figure S1 in Supporting Information S1). An updated composite stratigraphy and chronology is described in Supporting Information S1, and a detailed stratigraphic description is in Zander, Żarczyński, Vogel, et al. (2021). For the most recent  $\sim 2000$  years, the chronology is based on varve counting (Bonk, Tylmann, Goslar, et al., 2015; Zander, Żarczyński, Tylmann, et al., 2021; Żarczyński et al., 2018). New for this study, the Banded Age Model (Comboul et al., 2014) was used to calculate an ensemble of age-depth relationships for this upper section, via the R package *geoChronR* v1.1 (McKay et al., 2021); this enables the use of *geoChronR* to explore the effect of age uncertainty on correlations with instrumental and other proxy data. A mass movement deposit dated to  $\sim 2030$  cal yr BP precludes a continuous varve count tied to the surface. For sediments older than this deposit, an age model was constructed in OxCal v4.3 using a P-sequence (Bronk Ramsey, 2008, 2009; Bronk Ramsey & Lee, 2013). The P-sequence input includes 66 radiocarbon ages and two segments of floating varve counts ( $\sim 4,640$  and  $\sim 600$  varves, respectively).

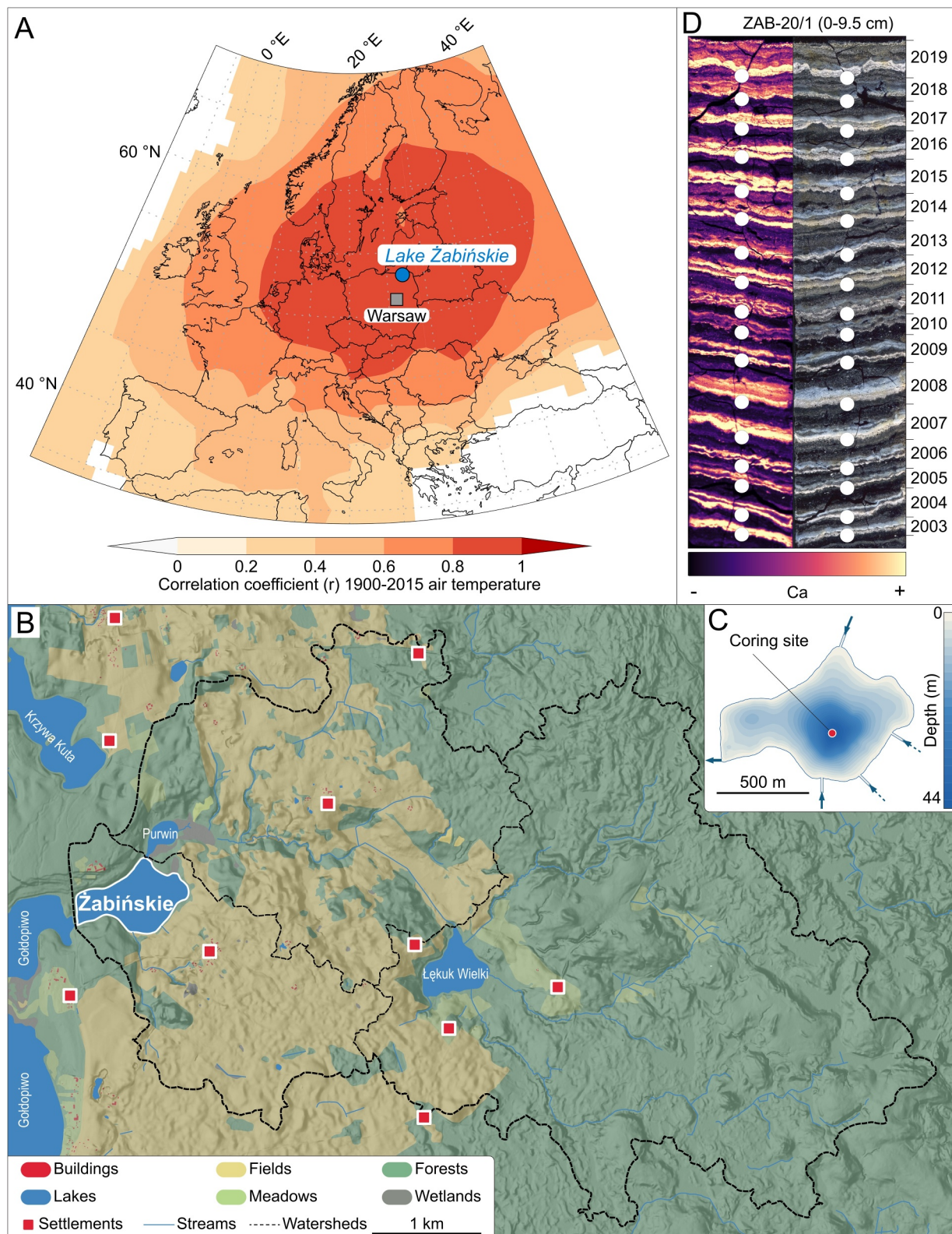


**Figure 1.** Study site. (a) Correlation map of annual air temperature with annual air temperature at Lake Żabińskie from 1900 to 2015. Map created using KNMI Climate Explorer (Trouet & Oldenborgh, 2013) with data from NOAA twentieth Century Reanalysis V3 (Compo et al., 2011; Slivinski et al., 2019). (b) Map of the Lake Żabińskie catchment (elevation data from Polish Head Office of Geodesy and Cartography). (c) Bathymetric map. (d) Top 9.5 cm of sediments with varve years labeled. Left shows Ca relative abundance based on  $\mu$ XRF imaging. Right is a scan of a thin section (cross-polarized light).

### 2.3. XRF Analysis

XRF elemental data were obtained in three measurement campaigns. Sediments older than 1.97 kyr BP were scanned at the University of Bern using an ITRAX core scanner (Cox Analytical Systems) with a Cr-tube (exposure time 20 s, 30 kV, 50 mA); the measurement resolution was 2 mm (Zander, Żarczyński, Vogel, et al., 2021). Sediments younger than 1.97 kyr BP were scanned at the University of Bremen with an ITRAX scanner with a Mo-tube (exposure time 10 s, 30 kV, 18 mA); the measurement resolution was 0.2 mm (Bonk et al., 2016; Żarczyński et al., 2019). For sediments deposited after 1966 CE, resin-embedded blocks were scanned with a Bruker M4 Tornado equipped with a Rh tube (exposure time 20 ms/pixel, 20  $\mu$ m spot size, 50 kV, 300  $\mu$ A) to produce spatial maps of elemental counts at 0.06 mm resolution (Zander, Żarczyński, Tylmann, et al., 2021). We use  $\ln(\text{Ca}/\text{Ti})$  as a temperature proxy. By normalizing with Ti, we attempt to isolate the signal of calcite that precipitates in the water column and correct for catchment-derived Ca. Log-ratios of XRF elemental ratios have been shown to correlate strongly with elemental concentrations (Bertrand et al., 2023; Weltje & Tjallingii, 2008). The three XRF data sets were homogenized by scaling  $\ln(\text{Ca}/\text{Ti})$  and other common elements such that overlapping sections of each data set have the same mean and variance after averaging into 3-year bins (more details in the Supporting Information S1).

### 2.4. Data Analysis

Data analysis was conducted with R v 4.2.3 (R Core Team, 2022). Proxy and geochronological data were input to a Linked PaleoData file (LiPD) (McKay & Emile-Geay, 2016) to be operable with *geoChronR*. Outliers were identified in the  $\ln(\text{Ca}/\text{Ti})$  data by applying a moving window filter of 100 years where values less than  $1.5 \times \text{IQR} - \text{Q1}$  or greater than  $1.5 \times \text{IQR} - \text{Q3}$  are considered outliers (IQR = interquartile range; Q1 and Q3 are first and third quartiles). Outliers were replaced with the threshold used to identify them. A large shift in  $\ln(\text{Ca}/\text{Ti})$  occurs in the eighteenth century due to the development of intensive agriculture in the catchment (Wacnik et al., 2016) and subsequently higher erosion rates (Bonk et al., 2016) (Figure S4 in Supporting Information S1). The *changePoint* package (Killick & Eckley, 2014) was used to find the breakpoint in mean values during the past 2000 years. The resulting breakpoint in 1730 CE is consistent with previous analyses of sedimentological and geochemical changes in response to human activity at this site (Bonk et al., 2016). To create a data set that can be used for paleoclimate reconstruction, we homogenized the data set with the assumption that sediment deposited 200 years before and after the breakpoint have the same mean  $\ln(\text{Ca}/\text{Ti})$ . This assumption implies that despite a large shift in the mean Ca/Ti values, the change in  $\ln(\text{Ca}/\text{Ti})$  per degree  $^{\circ}\text{C}$  of temperature change remained constant. This correction makes interpretation of absolute temperature values prior to 1730 CE uncertain but preserves high frequency variability in the record.

Age-uncertain correlation analysis was conducted using *geoChronR* (McKay et al., 2021). We tested the significance of a linear correlation between  $\ln(\text{Ca}/\text{Ti})$  and spring and summer (March to August; MAMJJA) temperatures at Warsaw (52.22 $^{\circ}$  N, 21.03 $^{\circ}$  E). Instrumental temperature records from Warsaw begin in 1779 CE (Lorenc, 2000). Additional data from 2000 to 2019 CE were obtained from the Polish Institute of Meteorology and Water Management using the *climate* package (Czernecki et al., 2020). Temperature anomalies were calculated relative to the period 1850–1900 CE. Proxy and instrumental data were binned into 3-year intervals. All correlations were calculated using an ensemble of 1,000 age model iterations to calculate a distribution of correlation statistics. Pearson's  $r$  was calculated to determine the strength of linear correlations. P-values were adjusted to account for autocorrelation using the effective- $n$  method (Dawdy & Matalas, 1964; McKay et al., 2021) and were adjusted for multiple hypothesis testing using the false discovery rate method (Benjamini & Hochberg, 1995). To reconstruct temperatures, the  $\ln(\text{Ca}/\text{Ti})$  values were scaled to match the mean and variance of the temperature time series over the instrumental period (1779–2019 CE). Scaling is favored over linear regression because it matches the variability of the reconstruction to the variability of the instrumental data (Esper et al., 2005). The scaling calculation was done for each age model ensemble, thereby propagating the uncertainty derived from age uncertainty through the scaling parameters. The root mean square error of prediction (RMSE) and reduction of error (RE; Cook et al., 1994) were calculated using a split-period validation approach in which the data were split in half into a calibration period and validation period; the periods were also switched. The RE and RMSE were calculated as 90% confidence intervals (CI) based on 1,000 model iterations for each split period.

Bandpass filters were applied to the reconstruction using the *signal* package (Mersmann et al., 2023). The wavelet power spectrum was calculated by applying a Morlet wavelet using *WaveletComp* (Roesch & Schmidbauer, 2018).

The significance of the wavelet power was assessed by comparing the wavelet spectrum with simulated time series ( $n = 1,000$ ) using an autoregressive AR(1) model. A time-averaged periodogram was calculated using the multitaper method with the package *astrochron* (Meyers, 2014).

### 3. Results and Discussion

#### 3.1. Calibration With Instrumental Data

The correlation between  $\ln(\text{Ca}/\text{Ti})$  and instrumental spring/summer (MAMJJA) temperatures is significant ( $p < 0.05$ ) in more than 99% of age model iterations, with  $r = 0.34\text{--}0.55$  (90% CI) (Figure 2). Because the varve count chronology is very precise over the instrumental period, age uncertainty has a minor effect on the slope observed in the linear regression of the two variables (Figure 2). The cross-validated RMSE is  $0.58\text{--}1.32^\circ\text{C}$ ; RE is  $0.00\text{--}0.52$  (positive values indicate the reconstruction has skill). The significant correlation confirms that the strong link between warm-season air temperature, epilimnion temperature and calcite precipitation observed in the modern lake (Żarczyński et al., 2022) was persistent since 1779 CE (beginning of the instrumental period), and we assume this relationship held throughout the Holocene. The close connection between warm-season temperature and calcite precipitation has been observed in other temperate hard-water lakes (Boyll et al., 2023; Escoffier et al., 2023; Hodell et al., 1998; Roeser et al., 2021). Typical for climate proxies, non-climatic factors can affect the proxy; these factors are discussed in detail in the Supporting Information S1.

We further validate the temperature reconstruction by correlation with an independent summer temperature reconstruction for Europe based on tree rings and historical documents (Luterbacher et al., 2016). We find significant correlations using either 30-year bins ( $r = 0.39\text{--}0.45$ , 98.6% of iterations significant) or three-year bins ( $r = 0.21\text{--}0.26$ , 100% significant). The central tendency of the Lake Żabińskie temperature anomalies and amplitude of variability are similar to the Luterbacher reconstruction, suggesting the homogenization approach used to account for the impact of increased erosion due to human activity was reasonable and that temperature-Ca/Ti relationship followed a similar scaling despite the mean shift at 1730 CE. The homogenization step has no impact on the calibration statistics or amplitude of variability but does affect the level of temperature anomalies before 1730 CE.

#### 3.2. Holocene Temperature Evolution

The millennial-scale trend of the Lake Żabińskie reconstruction agrees with northern hemisphere Holocene temperature reconstructions; in particular, there is strong agreement with Greenland  $\delta^{18}\text{O}$  (Figure 3). The early Holocene is defined by a warming trend as ice sheets retreated and the climate transitioned from a glacial to interglacial state. Maximal summer warmth occurs during the early Holocene, between 8.5 and 8.1 kyr BP, earlier than global proxy compilations (Erb et al., 2022; Kaufman, McKay, Routson, Erb, Dätwyler, et al., 2020) and pollen-based temperature estimates from northern Europe (Herzschuh et al., 2023), which both show the HTM around 7.5–6.0 kyr BP. However, the lagged response of vegetation equilibrium to climate change during the early Holocene likely leads to a cold bias in pollen temperature reconstructions (Dallmeyer et al., 2022; Väliranta et al., 2015). Geochemical proxies and aquatic macrofossils tend to show warmer temperatures during the early Holocene compared to pollen (Kaufman, McKay, Routson, Erb, Davis, et al., 2020), and marine proxies from the northern hemisphere also show an early Holocene HTM (Cartapanis et al., 2022). The warmest temperatures of the HTM are comparable to modern summer temperatures; however, absolute comparisons are possibly hampered by uncertainty associated with the data homogenization used to correct for anthropogenic erosion impacts to the  $\ln(\text{Ca}/\text{Ti})$  data.

Immediately following peak warmth, a dramatic  $\sim 2^\circ\text{C}$  cooling occurs, attributed to the “8.2 kyr event” (Alley et al., 1997; Thomas et al., 2007). The magnitude of cooling is broadly similar to other proxy estimates of this cold event from Europe and Greenland (Morrill et al., 2013). The cooling occurs slightly later in our chronology (Figure S5 in Supporting Information S1) (temperature minimum at 8,110–7,954 cal yr BP,  $2\sigma$ ) compared to the GICC05 Greenland ice core chronology (8,206–8,112 cal yr BP) (Gkinis et al., 2014; Rasmussen et al., 2022). The age offset is plausible given that this section of core has poorly preserved varves, and the age model relies on interpolation between radiocarbon ages.

From 7.5 to 4.7 kyr BP spring and summer temperatures were generally warm and stable, coinciding with the HTM observed in many European paleoecological proxies (Figure 3; Heiri et al., 2015; Herzschuh et al., 2023). A

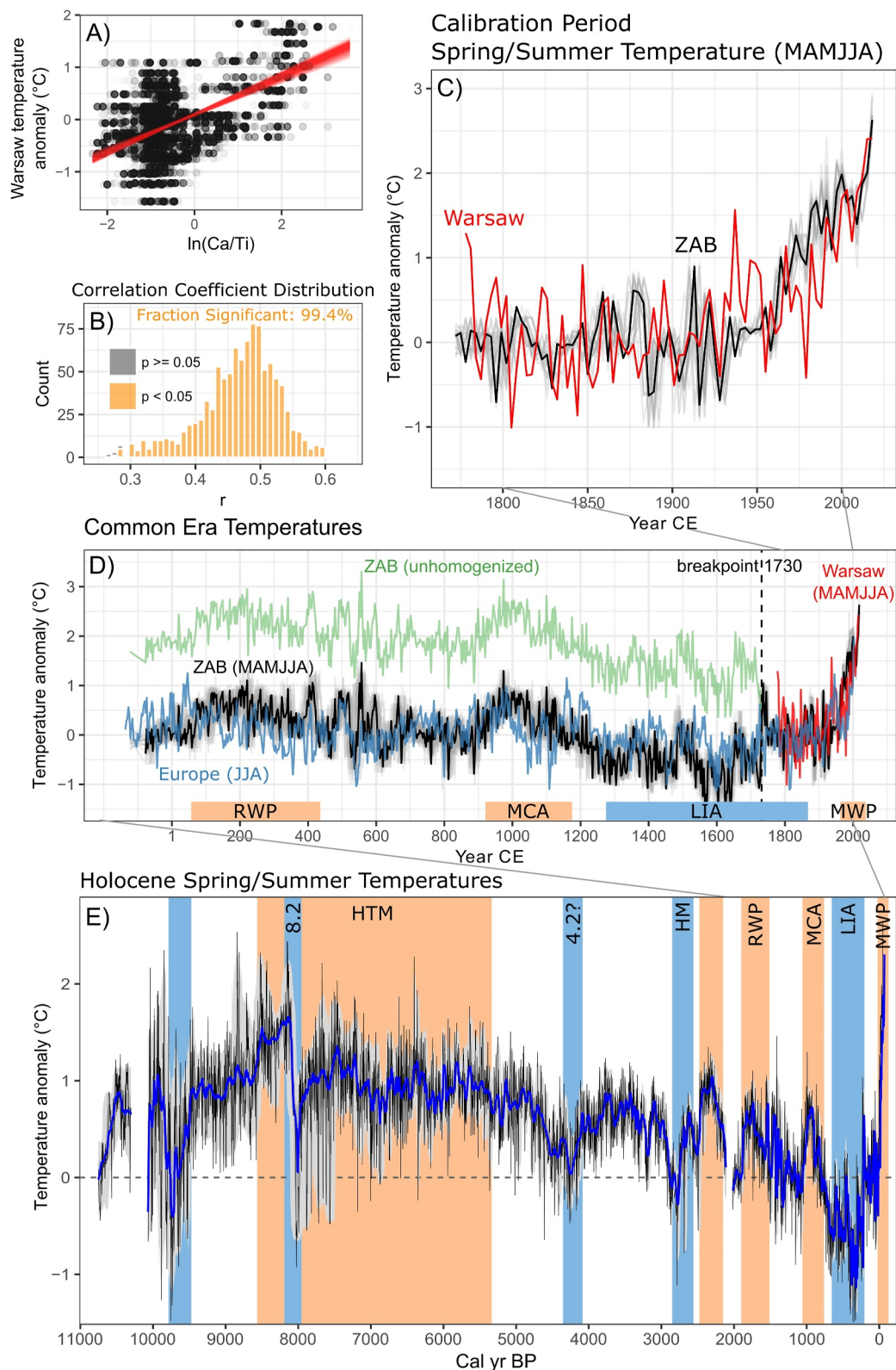


Figure 2.

long-term cooling trend is observed from 7.5 kyr BP to 1600 CE, likely driven by declining summer insolation in the northern hemisphere (Laskar et al., 2004). This cooling trend is punctuated by several pronounced fluctuations after 4.2 kyr BP (Figure 2). Cooling at 4.2 kyr BP is concurrent with a widespread drought/cold period that marks the Middle-Late Holocene boundary (Walker et al., 2012). However, the 4.2 kyr event is not widely recognized in central or northern Europe (Bradley & Bakke, 2019; Pleskot et al., 2020; Roland et al., 2014). Cooling at 2.8 kyr BP is likely caused by the Homeric solar minimum, associated with cool/stormy conditions in western Europe (Martin-Puertas et al., 2012; Rach et al., 2017) and widespread glacier advances in the Alps (Schimmelpfennig et al., 2022). Warm periods occur around 2.3 kyr BP, 50–400 CE Roman Warm Period (RWP; Ljungqvist, 2010), and 900–1200 CE Medieval Climate Anomaly (MCA; Mann et al., 2009). The RWP is widely recognized in the Mediterranean (Margaritelli et al., 2020), and there is also evidence for warmer conditions in Poland during the RWP (Jach et al., 2017). Cold temperatures are observed during the Little Ice Age (LIA; 1250–1850 CE) as found throughout Europe (Wanner et al., 2022).

### 3.3. Warm-Season Temperature Variability and Rates of Change During the Holocene

The continuous wavelet shows the greatest spectral power from 10 to 6.3 kyr BP, and lower spectral power after 6 kyr BP (Figure 4a). Decadal-scale periodicities are significant mainly during 10–6.3 kyr BP and the past 1800 years; the time-averaged multi-taper spectrum confirms that decadal periodicities are significant (Figure S7 in Supporting Information S1). Bandpass-filtered data show greater decadal to multidecadal variability from 10 to 7 kyr BP and especially high centennial-scale variability around 9–7 kyr BP (Figures 4c and 4d). This interval overlaps with the thermal maximum (orange bar in Figure 4b), but also includes the 8.2 ka event, which is the largest centennial-scale temperature swing in the record. Interestingly, enhanced decadal-to centennial-scale variability begins ~800 years before the onset of that event, and persists for ~500 years after. Running standard deviations ( $\sigma$ ) (90-year window) are highest around 10.0–9.4 and 8.2–7.5 kyr BP (Figure 4i), bracketing the temperature peak. The Lake Żabińskie record contrasts with that of Diss Mere, UK (Martin-Puertas et al., 2023), which shows dampened decadal periodicity from 8.5 to 6.7 kyr BP, attributed to changes in North Atlantic circulation. This discrepancy demonstrates that decadal-scale climate variability is regionally specific. However, this interval was relatively cool at Diss Mere, and when summer temperatures peaked around 4–5 kyr BP, decadal-scale variability increased (Martin-Puertas et al., 2023). The Diss Mere record and a high-resolution warm-season temperature proxy record from Germany (Sirocko et al., 2021) both support the pattern observed at Lake Żabińskie of greater decadal to multi-decadal variability of summer temperatures during warm climate phases.

Greater interannual to decadal variability during the HTM could be evidence of land-atmosphere feedbacks related to soil moisture that have been shown to increase interannual summer temperature variability at higher temperatures in this region during ongoing climate warming (Schär et al., 2004; Seneviratne et al., 2006). This effect would have been enhanced by the drier conditions of the early Holocene (Herzschuh et al., 2023), whereas wetter conditions after ca. 7.5 kyr BP likely reduced warm-season temperature variability through greater soil moisture (Fischer et al., 2012). Figure 4h shows a modest positive correlation between warm-season temperature and  $\sigma$ , but the greatest variability occurred at moderate temperatures, while the period of warmest temperatures (8.5–8.1 kyr BP) featured relatively low variability. Thus, the relationship between mean temperature and temperature variability is not a straightforward linear relationship. An additional mechanism that likely influenced decadal to centennial variability is volcanic activity, which was greater during the early Holocene and quieted after about 6–5 kyr BP (Figure 3g; Sigl et al., 2022; van Dijk et al., 2024).

To put modern warming rates in the context of the Holocene record, we calculated running 90-year linear trends. The median reconstructed warming rate during the past 90 years is 0.28°C/decade. The most recent period is the

**Figure 2.** Results of age-uncertain calibration-in-time using *geoChronR* (McKay et al., 2021). (a) Crossplot of  $\ln(\text{Ca}/\text{Ti})$  proxy data and instrumental spring/summer (March–August) temperature anomalies (relative to 1850–1900 CE) in Warsaw. (b) Histogram of Pearson's  $r$  correlation coefficients across age-model ensembles. (c) Comparison of instrumental temperatures (red) and Lake Żabińskie temperature reconstruction (3-year bins for both data sets). Black represents the median age model. Gray lines show 30 example age model iterations. (d) Lake Żabińskie temperature reconstruction compared to summer temperature reconstruction for Europe (light blue; 3-year bins) (Luterbacher et al., 2016). The green line shows the temperature reconstruction without homogenization to account for increased erosion in the eighteenth century. Other colors are the same as panel (c). (e) Holocene temperature reconstruction with major climate events labeled. The blue line indicates the median value for each three-year interval from 1,000 age-model iterations. The black line is the reconstruction plotted on the median age model. Gray shadings indicate 50% and 95% confidence intervals considering age uncertainty. HTM = Holocene Thermal Maximum, HM = Homer Minimum, RWP = Roman Warm Period, MCA = Medieval Climate Anomaly, LIA = Little Ice Age, MWP = Modern Warm Period.

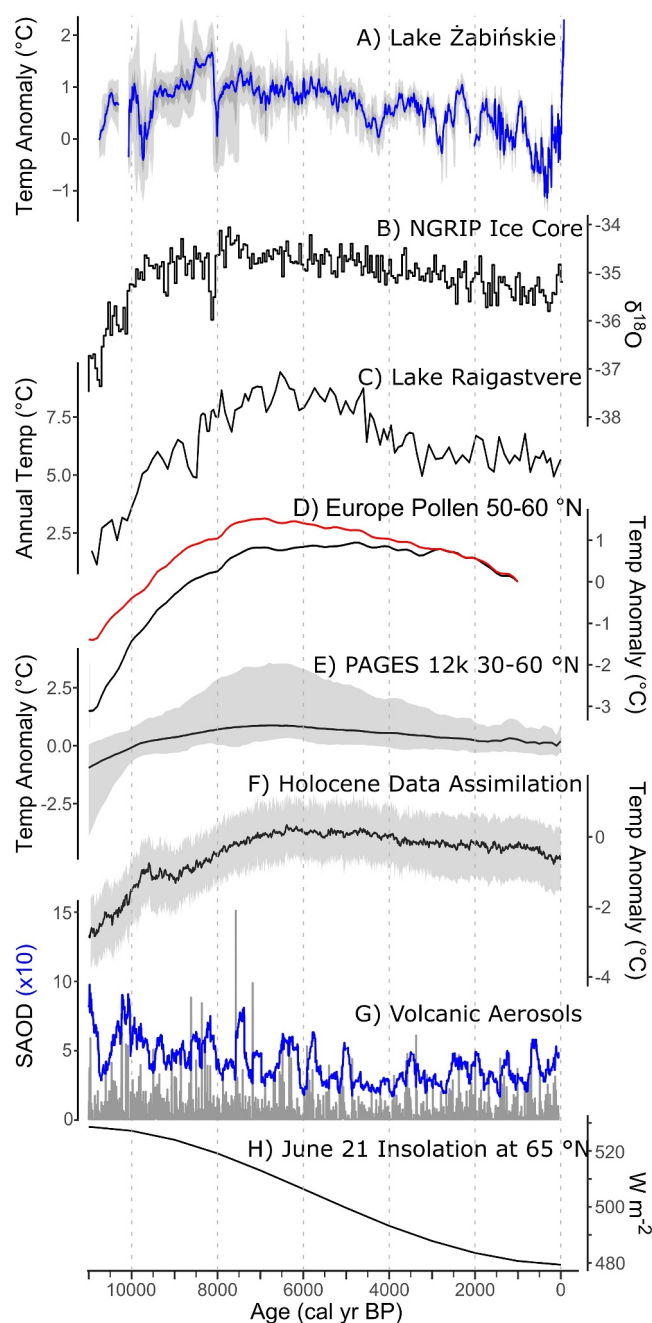


**Figure 3.** Comparison of Lake Žabińskie temperature reconstruction with relevant paleoclimate data and climate forcings. (a) Lake Žabińskie temperature reconstruction. Colors are defined as in Figure 2e. (b)  $\delta^{18}\text{O}$  from NGRIP ice core (Rasmussen et al., 2014). (c) Pollen-based annual temperature reconstruction from Lake Raigastvere, Estonia (Sundqvist et al., 2014). (d) Pollen-based annual (black) and July (red) temperature reconstruction for 50–60° N latitude in Europe (Herzschuh et al., 2023). (e) Annual temperature reconstruction for 30–60° N from the Temp12k compilation (Kaufman, McKay, Routson, Erb, Dätwyler, et al., 2020). (f) Annual temperature reconstruction for Lake Žabińskie grid point from Holocene Data Assimilation (Erb et al., 2022). (g) Northern Hemisphere Stratospheric Aerosol Optical Depth (SAOD) reconstruction from ice cores (Sigl et al., 2022). Plot shows annual sums (gray) and running 200-year sums (blue; scale is 10× the plotted scale). (h) Summer insolation at 65° N (Laskar et al., 2004).

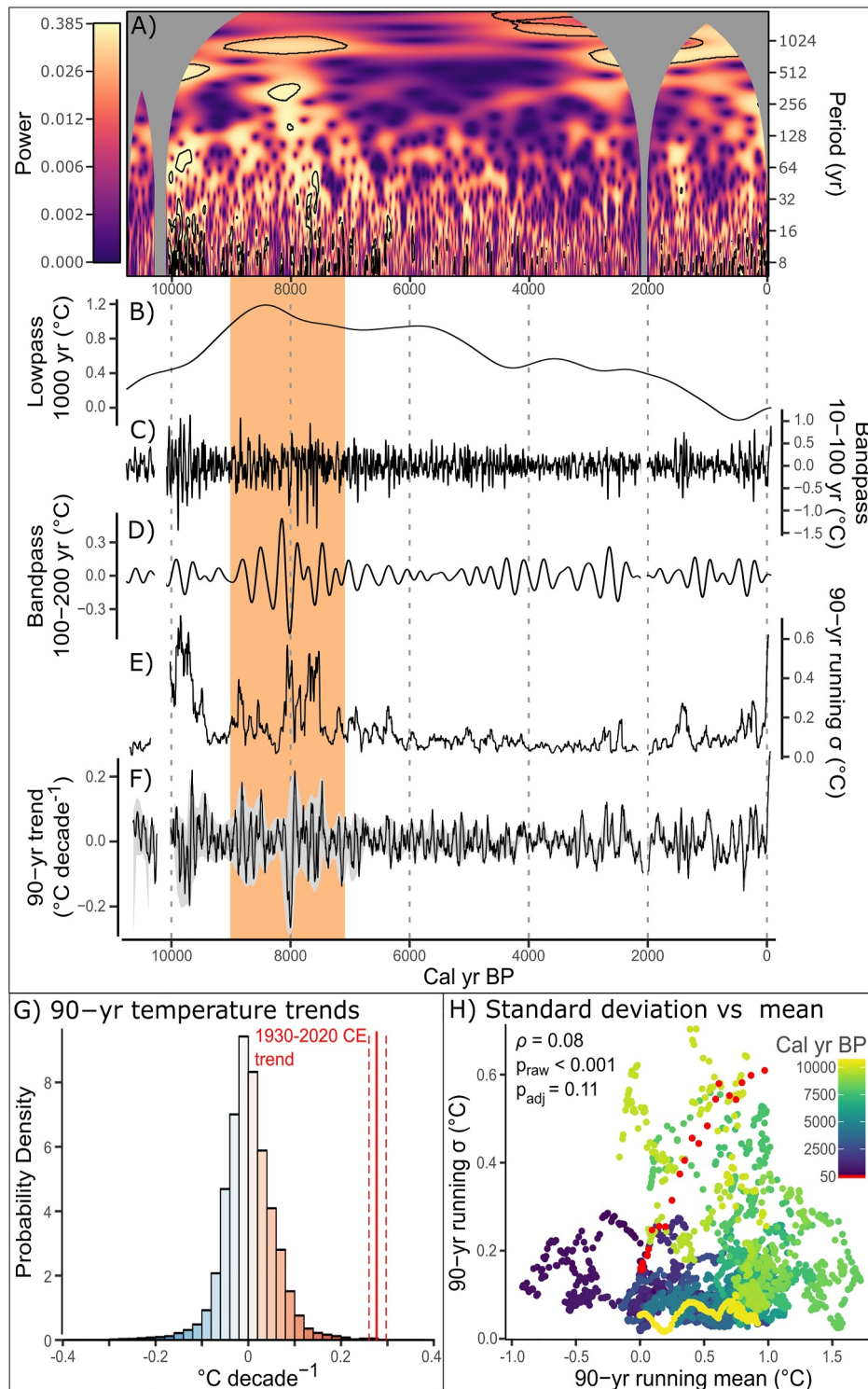


**Figure 4.** Holocene warm-season temperature variability and spectral analysis. (a) Continuous wavelet spectrum. Areas of significant periodicities are outlined in black; gray areas indicate data gaps and associated cones of influence. (b) 1,000-year lowpass-filtered temperature anomaly reconstruction showing multimillennial-scale trends. (c) 10–100-year bandpass-filtered data (decadal-to centennial-scale variability), (d) 100–200-year bandpass-filtered data (centennial-to multicentennial-scale variability). (e) 90-year running  $\sigma$  of the temperature reconstruction. (f) Temperature trends calculated for rolling 90-year intervals, gray shading indicates 95% confidence intervals (CI) of age ensemble. (g) Histogram of 90-year temperature trends (same data as F). The median trend of the most recent 90-year period in the reconstruction is marked by a red line (dashed lines represent 95% CI considering age uncertainty). (h) Cross-plot of temperature and  $\sigma$  using running 90-year windows.  $\rho$  is Spearman's rho and  $p_{\text{raw}}$  and  $p_{\text{adj}}$  are p-values without and with correction for autocorrelation, respectively.

fastest warming of the entire record in 84% of age model iterations and is more extreme than 99.96% of 90-year periods in the full reconstruction ensemble, representing 4.5–5.4 standard deviations beyond the mean (Figures 4f and 4g). This result is consistent with previous work comparing modern warming with paleoclimate data spanning the past 24,000 years (Osman et al., 2021), and has important implications for ecological adaptation to modern warming.

#### 4. Conclusions

We use a calibration-in-time method to reconstruct spring and summer temperature anomalies in northeastern Poland based on Ca/Ti ratios, a proxy for endogenic calcite. The 10,800-year reconstruction is unique for its length and resolution (three years), and provides important insights about high-frequency paleoclimate variability in this region, while also capturing long-term millennial-scale trends. The HTM occurs early in our record (8.5–8.1 kyr BP) and warm-season temperatures subsequently decline, indicating a strong influence of summer insolation. Temperature variability is greatest during the early Holocene, which is likely driven by land-atmosphere feedback processes, which were enhanced by drier conditions in the early Holocene. Greater volcanic activity may have also contributed to increased variability at this time. The rate of temperature change during the past 90 years at this site is most likely unprecedented in the Holocene.

#### Data Availability Statement

Data used in this study are archived at the NOAA National Centers for Environmental Information, under the World Data Service for Paleoclimatology (Zander et al., 2024; <https://doi.org/10.25921/tvqz-hz83>).

#### Acknowledgments

This project was funded by Swiss National Science Foundation Grants 200021\_172586 and P500PN\_206731, and Polish National Science Centre Grants 2014/13/B/ST10/01311 and 2015/18/E/ST10/00325. We thank Dirk Enters and Shauna-kay Rainford for their contributions. Open Access funding enabled and organized by Projekt DEAL.

#### References

- Alley, R. B., Mayewski, P. A., Sowers, T., Stuiver, M., Taylor, K. C., & Clark, P. U. (1997). Holocene climatic instability: A prominent, widespread event 8200 yr ago. *Geology*, 25(6), 483–486. [https://doi.org/10.1130/0091-7613\(1997\)025<0483:HCIAPW>2.3.CO;2](https://doi.org/10.1130/0091-7613(1997)025<0483:HCIAPW>2.3.CO;2)
- Benjamini, Y., & Hochberg, Y. (1995). Controlling the false discovery rate: A practical and powerful approach to multiple testing. *Journal of the Royal Statistical Society: Series B*, 57(1), 289–300. <https://doi.org/10.1111/j.2517-6161.1995.tb02031.x>
- Bertrand, S., Tjallingii, R., Kylander, M. E., Wilhelm, B., Roberts, S. J., Arnaud, F., et al. (2023). Inorganic geochemistry of lake sediments: A review of analytical techniques and guidelines for data interpretation. *Earth-Science Reviews*, 249, 104639. <https://doi.org/10.1016/j.earscirev.2023.104639>
- Bonk, A., Kinder, M., Enters, D., Grosjean, M., Meyer-Jacob, C., & Tylmann, W. (2016). Sedimentological and geochemical responses of Lake Żabińskie (north-eastern Poland) to erosion changes during the last millennium. *Journal of Paleolimnology*, 56(2–3), 239–252. <https://doi.org/10.1007/s10933-016-9910-6>
- Bonk, A., Tylmann, W., Amann, B., Enters, D., & Grosjean, M. (2015). Modern limnology and varve-formation processes in lake Żabińskie, northeastern Poland: Comprehensive process studies as a key to understand the sediment record. *Journal of Limnology*, 74(2), 358–370. <https://doi.org/10.4081/jlimnol.2014.1117>
- Bonk, A., Tylmann, W., Goslar, T., Wacnik, A., & Grosjean, M. (2015). Comparing varve counting and 14C-Ams chronologies in the sediments of Lake Żabińskie, Northeastern Poland: Implications for accurate 14C dating of lake sediments. *Geochronometria*, 42(1), 157–171. <https://doi.org/10.1515/geochr-2015-0019>
- Bova, S., Rosenthal, Y., Liu, Z., Godad, S. P., & Yan, M. (2021). Seasonal origin of the thermal maxima at the Holocene and the last interglacial. *Nature*, 589(7843), 548–553. <https://doi.org/10.1038/s41586-020-03155-x>
- Boyll, L., Valcárcel, J. I., Harding, P., Hernández, A., & Martin-Puertas, C. (2023). Disentangling the environmental signals recorded in Holocene calcite varves based on modern lake observations and annual sedimentary processes in Diss Mere, England. *Journal of Paleolimnology*, 70(1), 39–56. <https://doi.org/10.1007/s10933-023-00282-z>
- Bradley, R. S., & Bakke, J. (2019). Is there evidence for a 4.2 ka BP event in the northern North Atlantic region? *Climate of the Past*, 15(5), 1665–1676. <https://doi.org/10.5194/cp-15-1665-2019>
- Brauer, A., Dulski, P., Mangili, C., Mingram, J., & Liu, J. (2009). The potential of varves in high-resolution paleolimnological studies. *PAGES News*, 17(3), 96–98. <https://doi.org/10.22498/pages.17.3.96>
- Bronk Ramsey, C. (2008). Deposition models for chronological records. *Quaternary Science Reviews*, 27(1–2), 42–60. <https://doi.org/10.1016/j.quascirev.2007.01.019>
- Bronk Ramsey, C. (2009). Bayesian analysis of radiocarbon dates. *Radiocarbon*, 51(1), 337–360. <https://doi.org/10.1017/s0033822200033865>
- Bronk Ramsey, C., & Lee, S. (2013). Recent and planned developments of the program OxCal. *Radiocarbon*, 55(2), 720–730. <https://doi.org/10.1017/s0033822200057878>
- Cartapanis, O., Jonkers, L., Moffa-Sanchez, P., Jaccard, S. L., & de Vernal, A. (2022). Complex spatio-temporal structure of the Holocene Thermal Maximum. *Nature Communications*, 13(1), 5662. <https://doi.org/10.1038/s41467-022-33362-1>
- Comboul, M., Emile-Geay, J., Evans, M. N., Mirmateghi, N., Cobb, K. M., & Thompson, D. M. (2014). A probabilistic model of chronological errors in layer-counted climate proxies: Applications to annually banded coral archives. *Climate of the Past*, 10(2), 825–841. <https://doi.org/10.5194/CP-10-825-2014>
- Compo, G. P., Whitaker, J. S., Sardeshmukh, P. D., Matsui, N., Allan, R. J., Yin, X., et al. (2011). The twentieth century reanalysis project. *Quarterly Journal of the Royal Meteorological Society*, 137(654), 1–28. <https://doi.org/10.1002/qj.776>
- Cook, E. R., Briffa, K. R., & Jones, P. D. (1994). Spatial regression methods in dendroclimatology: A review and comparison of two techniques. *International Journal of Climatology*, 14(4), 379–402. <https://doi.org/10.1002/joc.3370140404>

- Czernecki, B., Glogowski, A., & Nowosad, J. (2020). Climate: An R package to access free in-situ meteorological and hydrological datasets for environmental assessment. *Sustainability*, *12*(1), 394. <https://doi.org/10.3390/su12010394>
- Dallmeyer, A., Kleinen, T., Claussen, M., Weitzel, N., Cao, X., & Herzschuh, U. (2022). The deglacial forest conundrum. *Nature Communications*, *13*(1), 6035. <https://doi.org/10.1038/s41467-022-33646-6>
- Dawdy, D., & Matalas, N. (1964). Analysis of variance, covariance, and time series. In V. Chow (Ed.), *Handbook of applied hydrology* (pp. 8–68–8–90). McGraw-Hill Book Co.
- Erb, M. P., McKay, N. P., Steiger, N., Dee, S., Hancock, C., Ivanovic, R. F., et al. (2022). Reconstructing Holocene temperatures in time and space using paleoclimate data assimilation. *Climate of the Past*, *18*(12), 2599–2629. <https://doi.org/10.5194/cp-18-2599-2022>
- Escoffier, N., Perolo, P., Many, G., Pasche, N. T., & Perga, M.-E. (2023). Fine-scale dynamics of calcite precipitation in a large hardwater lake. *Science of the Total Environment*, *864*, 160699. <https://doi.org/10.1016/j.scitotenv.2022.160699>
- Esper, J., Frank, D. C., Wilson, R. J. S., & Briffa, K. R. (2005). Effect of scaling and regression on reconstructed temperature amplitude for the past millennium. *Geophysical Research Letters*, *32*(7), 2004GL021236. <https://doi.org/10.1029/2004GL021236>
- Essell, H., Krusic, P. J., Esper, J., Wagner, S., Braconnot, P., Jungclauss, J., et al. (2023). A frequency-optimised temperature record for the Holocene. *Environmental Research Letters*, *18*(11), 114022. <https://doi.org/10.1088/1748-9326/ad0065>
- Fischer, E. M., Rajczak, J., & Schär, C. (2012). Changes in European summer temperature variability revisited. *Geophysical Research Letters*, *39*(19). <https://doi.org/10.1029/2012GL052730>
- Gkinis, V., Simonsen, S. B., Buchardt, S. L., White, J. W. C., & Vinther, B. M. (2014). Water isotope diffusion rates from the NorthGRIP ice core for the last 16,000 years – Glaciological and paleoclimatic implications. *Earth and Planetary Science Letters*, *405*, 132–141. <https://doi.org/10.1016/j.epsl.2014.08.022>
- Heiri, O., Ilyashuk, B., Millet, L., Samartin, S., & Lotter, A. F. (2015). Stacking of discontinuous regional palaeoclimate records: Chironomid-based summer temperatures from the Alpine region. *The Holocene*, *25*(1), 137–149. <https://doi.org/10.1177/0959683614556382>
- Herzschuh, U., Böhmert, T., Chevalier, M., Hébert, R., Dallmeyer, A., Li, C., et al. (2023). Regional pollen-based Holocene temperature and precipitation patterns depart from the Northern Hemisphere mean trends. *Climate of the Past*, *19*(7), 1481–1506. <https://doi.org/10.5194/cp-19-1481-2023>
- Hodell, D. A., Schelske, C. L., Fahnenstiel, G. L., & Robbins, L. L. (1998). Biologically induced calcite and its isotopic composition in Lake Ontario. *Limnology & Oceanography*, *43*(2), 187–199. <https://doi.org/10.4319/lo.1998.43.2.0187>
- Jach, R., Knutelski, S., Uchman, A., Hercman, H., & Dohnalik, M. (2017). Subfossil markers of climate change during the Roman Warm Period of the late Holocene. *Science and Nature*, *105*(1), 6. <https://doi.org/10.1007/s00114-017-1533-x>
- Kaufman, D. S., & Broadman, E. (2023). Revisiting the Holocene global temperature conundrum. *Nature*, *614*(7948), 425–435. <https://doi.org/10.1038/s41586-022-05536-w>
- Kaufman, D. S., McKay, N., Routson, C., Erb, M., Dätwyler, C., Sommer, P. S., et al. (2020). Holocene global mean surface temperature, a multi-method reconstruction approach. *Scientific Data*, *7*(1), 1–13. <https://doi.org/10.1038/s41597-020-0530-7>
- Kaufman, D. S., McKay, N., Routson, C., Erb, M., Davis, B., Heiri, O., et al. (2020). A global database of Holocene paleotemperature records. *Scientific Data*, *7*(1), 1–34. <https://doi.org/10.1038/s41597-020-0445-3>
- Killick, R., & Eckley, I. A. (2014). ChangePoint: An R package for changepoint analysis. *Journal of Statistical Software*, *58*(3), 1–19. <https://doi.org/10.18637/jss.v058.i03>
- Lapointe, F., Bradley, R. S., Francus, P., Balascio, N. L., Abbott, M. B., Stoner, J. S., et al. (2020). Annually resolved Atlantic sea surface temperature variability over the past 2,900 y. *Proceedings of the National Academy of Sciences of the United States of America*, *117*(44), 27171–27178. <https://doi.org/10.1073/pnas.2014166117>
- Laskar, J., Robutel, P., Joutel, F., Gastineau, M., Correia, A. C. M., & Levrard, B. (2004). A long-term numerical solution for the insolation quantities of the Earth. *Astronomy & Astrophysics*, *428*(1), 261–285. <https://doi.org/10.1051/0004-6361:20041335>
- Liu, Z., Otto-Bliesner, B. L., He, F., Brady, E. C., Tomas, R., Clark, P. U., et al. (2009). Transient simulation of last deglaciation with a new mechanism for Bølling-Allerød warming. *Science*, *325*(5938), 310–314. <https://doi.org/10.1126/science.1171041>
- Liu, Z., Zhu, J., Rosenthal, Y., Zhang, X., Otto-Bliesner, B. L., Timmermann, A., et al. (2014). The Holocene temperature conundrum. *Proceedings of the National Academy of Sciences of the United States of America*, *111*(34), E3501–E3505. <https://doi.org/10.1073/pnas.1407229111>
- Ljungqvist, F. C. (2010). A new reconstruction of temperature variability in the extra-tropical northern hemisphere during the last two millennia. *Geografiska Annaler - Series A: Physical Geography*, *92*(3), 339–351. <https://doi.org/10.1111/j.1468-0459.2010.00399.x>
- Lorenc, H. (2000). *Serią temperatury powietrza w Warszawie oraz ocena jej wiekowych tendencji* (Vol. 31, p. 104). Materiały Badawcze IMGW.
- Luterbacher, J., Werner, J. P., Smerdon, J. E., Fernández-Donado, L., González-Rouco, F., J., Barriopedro, D., et al. (2016). European summer temperatures since Roman times. *Environmental Research Letters*, *11*(2), 024001. <https://doi.org/10.1088/1748-9326/11/2/024001>
- Mann, M. E., Zhang, Z., Rutherford, S., Bradley, R. S., Hughes, M. K., Shindell, D., et al. (2009). Global signatures and dynamical origins of the Little Ice Age and Medieval Climate Anomaly. *Science*, *326*(5957), 1256–1260. <https://doi.org/10.1126/science.1177303>
- Marcott, S. A., Shakun, J. D., Clark, P. U., & Mix, A. C. (2013). A reconstruction of regional and global temperature for the past 11,300 years. *Science*, *339*(6124), 1198–1201. <https://doi.org/10.1126/science.1228026>
- Margaritelli, G., Cacho, I., Català, A., Barra, M., Bellucci, L. G., Lubritto, C., et al. (2020). Persistent warm Mediterranean surface waters during the Roman period. *Scientific Reports*, *10*(1), 10431. <https://doi.org/10.1038/s41598-020-67281-2>
- Martin-Puertas, C., Hernandez, A., Pardo-Igúzquiza, E., Boyall, L., Brierley, C., Jiang, Z., et al. (2023). Dampened predictable decadal North Atlantic climate fluctuations due to ice melting. *Nature Geoscience*, *16*(4), 357–362. <https://doi.org/10.1038/s41561-023-01145-y>
- Martin-Puertas, C., Matthes, K., Brauer, A., Muscheler, R., Hansen, F., Petrick, C., et al. (2012). Regional atmospheric circulation shifts induced by a grand solar minimum. *Nature Geoscience*, *5*(6), 397–401. <https://doi.org/10.1038/ngeo1460>
- McKay, N. P., & Emile-Geay, J. (2016). Technical note: The Linked Paleo Data framework – A common tongue for paleoclimatology. *Climate of the Past*, *12*(4), 1093–1100. <https://doi.org/10.5194/cp-12-1093-2016>
- McKay, N. P., Emile-Geay, J., & Khider, D. (2021). GeoChronR – An R package to model, analyze, and visualize age-uncertain data. *Geochronology*, *3*(1), 149–169. <https://doi.org/10.5194/GCHRON-3-149-2021>
- Mersmann, O., Ligges, U., Krey, S., & Schnackenberg, S. (2023). Signal: Signal processing. Retrieved from <https://r-forge.r-project.org/projects/signal/>
- Meyers, S. R. (2014). Astrochron: An R package for astrochronology. Retrieved from <https://cran.r-project.org/package=astrochron>
- Morrill, C., Anderson, D. M., Bauer, B. A., Buckner, R., Gille, E. P., Gross, W. S., et al. (2013). Proxy benchmarks for intercomparison of 8.2 ka simulations. *Climate of the Past*, *9*(1), 423–432. <https://doi.org/10.5194/cp-9-423-2013>
- Osman, M. B., Tierney, J. E., Zhu, J., Tardif, R., Hakim, G. J., King, J., & Poulsen, C. J. (2021). Globally resolved surface temperatures since the Last Glacial Maximum. *Nature*, *599*(7884), 239–244. <https://doi.org/10.1038/s41586-021-03984-4>

- Pleskot, K., Apolinarska, K., Kolaczek, P., Suchora, M., Fojutowski, M., Joniak, T., et al. (2020). Searching for the 4.2 ka climate event at Lake Spore, Poland. *CATENA*, *191*, 104565. <https://doi.org/10.1016/j.catena.2020.104565>
- Rach, O., Engels, S., Kahmen, A., Brauer, A., Martín-Puertas, C., van Geel, B., & Sachse, D. (2017). Hydrological and ecological changes in western Europe between 3200 and 2000 years BP derived from lipid biomarker  $\delta D$  values in lake Meerfelder Maar sediments. *Quaternary Science Reviews*, *172*, 44–54. <https://doi.org/10.1016/j.quascirev.2017.07.019>
- Rasmussen, S. O., Bigler, M., Blockley, S. P., Blunier, T., Buchardt, S. L., Clausen, H. B., et al. (2014). A stratigraphic framework for abrupt climatic changes during the Last Glacial period based on three synchronized Greenland ice-core records: Refining and extending the INTIMATE event stratigraphy. *Quaternary Science Reviews*, *106*, 14–28. <https://doi.org/10.1016/j.quascirev.2014.09.007>
- Rasmussen, S. O., Svensson, A. M., & Vinther, B. M. (2022). Greenland Ice-Core Chronology 2005 (GICC05) annual layer depths for various Greenland ice cores [Dataset]. *PANGAEA*. <https://doi.org/10.1594/PANGAEA.943195>
- R Core Team. (2022). *R: A language and environment for statistical computing*. R Foundation for Statistical Computing. Retrieved from <https://www.r-project.org/>
- Roesch, A., & Schmidbauer, H. (2018). WaveletComp: Computational wavelet analysis. Retrieved from <https://CRAN.R-project.org/package=WaveletComp>
- Roeser, P., Dräger, N., Brykała, D., Ott, F., Pinkerneil, S., Gierszewski, P., et al. (2021). Advances in understanding calcite varve formation: New insights from a dual lake monitoring approach in the southern Baltic lowlands. *Boreas*, *50*(2), 419–440. <https://doi.org/10.1111/BOR.12506>
- Roland, T. P., Caseldine, C. J., Charman, D. J., Turney, C. S. M., & Amesbury, M. J. (2014). Was there a ‘4.2 ka event’ in Great Britain and Ireland? Evidence from the peatland record. *Quaternary Science Reviews*, *83*, 11–27. <https://doi.org/10.1016/j.quascirev.2013.10.024>
- Schär, C., Vidale, P. L., Lüthi, D., Frei, C., Häberli, C., Liniger, M. A., & Appenzeller, C. (2004). The role of increasing temperature variability in European summer heatwaves. *Nature*, *427*(6972), 332–336. <https://doi.org/10.1038/nature02300>
- Schimmelpfennig, I., Schaefer, J. M., Lamp, J., Godard, V., Schwartz, R., Bard, E., et al. (2022). Glacier response to Holocene warmth inferred from in situ Be and 14 C bedrock analyses in Steingletscher’s forefield (central Swiss Alps). *Climate of the Past*, *18*(1), 23–44. <https://doi.org/10.5194/cp-18-23-2022>
- Seneviratne, S. I., Lüthi, D., Litschi, M., & Schär, C. (2006). Land–atmosphere coupling and climate change in Europe. *Nature*, *443*(7108), 205–209. <https://doi.org/10.1038/nature05095>
- Sigl, M., Toohey, M., McConnell, J. R., Cole-Dai, J., & Severi, M. (2022). Volcanic stratospheric sulfur injections and aerosol optical depth during the Holocene (past 11 500 years) from a bipolar ice-core array. *Earth System Science Data*, *14*(7), 3167–3196. <https://doi.org/10.5194/essd-14-3167-2022>
- Sirocko, F., Martínez-García, A., Mudelsee, M., Albert, J., Britzjus, S., Christl, M., et al. (2021). Muted multidecadal climate variability in central Europe during cold stadial periods. *Nature Geoscience*, *14*(9), 651–658. <https://doi.org/10.1038/s41561-021-00786-1>
- Slivinski, L. C., Compo, G. P., Whitaker, J. S., Sardeshmukh, P. D., Giese, B. S., McColl, C., et al. (2019). Towards a more reliable historical reanalysis: Improvements for version 3 of the Twentieth Century Reanalysis system. *Quarterly Journal of the Royal Meteorological Society*, *145*(724), 2876–2908. <https://doi.org/10.1002/qj.3598>
- Stewart, M. M., Larocque-Tobler, L., & Grosjean, M. (2011). Quantitative inter-annual and decadal June–July–August temperature variability ca. 570 BC to AD 120 (Iron Age–Roman Period) reconstructed from the varved sediments of Lake Silvaplana, Switzerland. *Journal of Quaternary Science*, *26*(5), 491–501. <https://doi.org/10.1002/jqs.1480>
- Sundqvist, H. S., Kaufman, D. S., McKay, N. P., Balascio, N. L., Briner, J. P., Cwynar, L. C., et al. (2014). Arctic Holocene proxy climate database - New approaches to assessing geochronological accuracy and encoding climate variables. *Climate of the Past*, *10*(4), 1605–1631. <https://doi.org/10.5194/cp-10-1605-2014>
- Szymański, A. (2000). *Objaśnienia do Szczegółowej Mapy Geologicznej Polski, Arkusz Gózycko*, (Explanation to the detailed geological map of Poland, sheet Gózycko (104)). Polish Geological Institute.
- Thomas, E. R., Wolff, E. W., Mulvaney, R., Steffensen, J. P., Johnsen, S. J., Arrowsmith, C., et al. (2007). The 8.2ka event from Greenland ice cores. *Quaternary Science Reviews*, *26*(1), 70–81. <https://doi.org/10.1016/j.quascirev.2006.07.017>
- Tomczyk, A. M., & Bednorz, E. (Eds.). (2022). *Atlas klimatu Polski (1991-2020)*. Bogucki Wydawnictwo Naukowe.
- Trachsel, M., Eggenberger, U., Grosjean, M., Blass, A., & Sturm, M. (2008). Mineralogy-based quantitative precipitation and temperature reconstructions from annually laminated lake sediments (Swiss Alps) since AD 1580. *Geophysical Research Letters*, *35*(13), L13707. <https://doi.org/10.1029/2008GL034121>
- Trouet, V., & Oldenborgh, G. J. V. (2013). KNMI climate explorer: A web-based research tool for high-resolution paleoclimatology. *Tree-Ring Research*, *69*(1), 3–13. <https://doi.org/10.3959/1536-1098-69.1.3>
- Tylmann, W., Bonk, A., Borowiak, D., Głowacka, P., Nowiński, K., Piłczyńska, J., et al. (2023). Investigating limnological processes and modern sedimentation at Lake Żabińskie, northeast Poland: A decade-long multi-variable dataset, 2012–2021. *Earth System Science Data*, *15*(11), 5093–5103. <https://doi.org/10.5194/essd-15-5093-2023>
- Väliranta, M., Salonen, J. S., Heikkilä, M., Amon, L., Helmens, K., Klimaschewski, A., et al. (2015). Plant macrofossil evidence for an early onset of the Holocene summer thermal maximum in northernmost Europe. *Nature Communications*, *6*(1), 6809. <https://doi.org/10.1038/ncomms7809>
- van Dijk, E. J. C., Jungclauss, J., Sigl, M., Timmreck, C., & Krüger, K. (2024). High-frequency climate forcing causes prolonged cold periods in the Holocene. *Communications Earth & Environment*, *5*(1), 1–9. <https://doi.org/10.1038/s43247-024-01380-0>
- von Gunten, L., Grosjean, M., Kamenik, C., Fajak, M., & Urrutia, R. (2012). Calibrating biogeochemical and physical climate proxies from non-varved lake sediments with meteorological data: Methods and case studies. *Journal of Paleolimnology*, *47*(4), 583–600. <https://doi.org/10.1007/s10933-012-9582-9>
- Wacnik, A., Tylmann, W., Bonk, A., Goslar, T., Enters, D., Meyer-Jacob, C., & Grosjean, M. (2016). Determining the responses of vegetation to natural processes and human impacts in North-eastern Poland during the last millennium: Combined pollen, geochemical and historical data. *Vegetation History and Archaeobotany*, *25*(5), 479–498. <https://doi.org/10.1007/s00334-016-0565-z>
- Walker, M. J. C., Berkelhammer, M., Björck, S., Cwynar, L. C., Fisher, D. A., Long, A. J., et al. (2012). Formal subdivision of the Holocene series/epoch: A discussion paper by a working group of INTIMATE (integration of ice-core, marine and terrestrial records) and the Subcommission on Quaternary Stratigraphy (International Commission on Stratigraphy). *Journal of Quaternary Science*, *27*(7), 649–659. <https://doi.org/10.1002/jqs.2565>
- Wanner, H., Pfister, C., & Neukom, R. (2022). The variable European Little Ice Age. *Quaternary Science Reviews*, *287*, 107531. <https://doi.org/10.1016/j.quascirev.2022.107531>
- Weltje, G. J., & Tjallingii, R. (2008). Calibration of XRF core scanners for quantitative geochemical logging of sediment cores: Theory and application. *Earth and Planetary Science Letters*, *274*(3–4), 423–438. <https://doi.org/10.1016/j.epsl.2008.07.054>

- Zander, P. D., Szidat, S., Kaufman, D. S., Żarczyński, M., Poraj-Górska, A. I., Boltshauser-Kaltenrieder, P., & Grosjean, M. (2020). Miniature radiocarbon measurements (<150 µg C) from sediments of Lake Żabińskie, Poland: Effect of precision and dating density on age–depth models. *Geochronology*, 2(1), 63–79. <https://doi.org/10.5194/gchron-2-63-2020>
- Zander, P. D., Żarczyński, M., Tylmann, W., Rainford, S., & Grosjean, M. (2021). Seasonal climate signals preserved in biochemical varves: Insights from novel high-resolution sediment scanning techniques. *Climate of the Past*, 17(5), 2055–2071. <https://doi.org/10.5194/cp-17-2055-2021>
- Zander, P. D., Żarczyński, M., Tylmann, W., Vogel, H., & Grosjean, M. (2024). Temperature reconstruction, XRF data, and chronology, 10.8–0 kyr BP, Lake Żabińskie, Poland [Dataset]. NOAA National Centers for Environmental Information. <https://doi.org/10.25921/tvqz-hz83>
- Zander, P. D., Żarczyński, M., Vogel, H., Tylmann, W., Wacnik, A., Sanchini, A., & Grosjean, M. (2021). A high-resolution record of Holocene primary productivity and water-column mixing from the varved sediments of Lake Żabińskie, Poland. *Science of the Total Environment*, 755, 143713. <https://doi.org/10.1016/j.scitotenv.2020.143713>
- Żarczyński, M., Tylmann, W., & Goslar, T. (2018). Multiple varve chronologies for the last 2000 years from the sediments of Lake Żabińskie (northeastern Poland) – Comparison of strategies for varve counting and uncertainty estimations. *Quaternary Geochronology*, 47, 107–119. <https://doi.org/10.1016/j.quageo.2018.06.001>
- Żarczyński, M., Wacnik, A., & Tylmann, W. (2019). Tracing lake mixing and oxygenation regime using the Fe/Mn ratio in varved sediments: 2000 year-long record of human-induced changes from Lake Żabińskie (NE Poland). *Science of the Total Environment*, 657, 585–596. <https://doi.org/10.1016/j.scitotenv.2018.12.078>
- Żarczyński, M., Zander, P. D., Grosjean, M., & Tylmann, W. (2022). Linking the formation of varves in a eutrophic temperate lake to meteorological conditions and water column dynamics. *Science of the Total Environment*, 842, 156787. <https://doi.org/10.1016/J.SCITOTENV.2022.156787>
- Zolitschka, B., Francus, P., Ojala, A. E. K., & Schimmelmann, A. (2015). Varves in lake sediments - A review. *Quaternary Science Reviews*, 117, 1–41. <https://doi.org/10.1016/j.quascirev.2015.03.019>

## References From the Supporting Information

- Hernández-Almeida, I., Grosjean, M., Tylmann, W., & Bonk, A. (2015). Chrysophyte cyst-inferred variability of warm season lake water chemistry and climate in northern Poland: Training set and downcore reconstruction. *Journal of Paleolimnology*, 53(1), 123–138. <https://doi.org/10.1007/s10933-014-9812-4>
- Kinder, M., Wulf, S., Appelt, O., Hardiman, M., Żarczyński, M., & Tylmann, W. (2020). Late-Holocene ultra-distal cryptotephra discoveries in varved sediments of Lake Żabińskie, NE Poland. *Journal of Volcanology and Geothermal Research*, 402, 106988. <https://doi.org/10.1016/j.jvolgeores.2020.106988>
- O'Neill, B. C., Tebaldi, C., van Vuuren, D. P., Eyring, V., Friedlingstein, P., Hurtt, G., et al. (2016). The Scenario Model Intercomparison Project (ScenarioMIP) for CMIP6. *Geoscientific Model Development*, 9(9), 3461–3482. <https://doi.org/10.5194/gmd-9-3461-2016>
- Reimer, P. J., Austin, W. E. N., Bard, E., Bayliss, A., Blackwell, P. G., Bronk Ramsey, C., et al. (2020). The IntCal20 northern hemisphere radiocarbon age calibration curve (0–55 cal kBP). *Radiocarbon*, 62(4), 725–757. <https://doi.org/10.1017/RDC.2020.41>
- Stabel, H. H. (1986). Calcite precipitation in Lake Constance: Chemical equilibrium, sedimentation, and nucleation by algae. *Limnology & Oceanography*, 31(5), 1081–1094. <https://doi.org/10.4319/lo.1986.31.5.1081>
- Tylmann, W., Bonk, A., Goslar, T., Wulf, S., & Grosjean, M. (2016). Calibrating 210 Pb dating results with varve chronology and independent chronostratigraphic markers: Problems and implications. *Quaternary Geochronology*, 32, 1–10. <https://doi.org/10.1016/j.quageo.2015.11.004>
- Witak, M., Hernández-Almeida, I., Grosjean, M., & Tylmann, W. (2017). Diatom-based reconstruction of trophic status changes recorded in varved sediments of Lake Żabińskie (northeastern Poland), AD 1888–2010. *Oceanological and Hydrobiological Studies*, 46(1), 1–17. <https://doi.org/10.1515/ohs-2017-0001>